Binary Structure in Time Distributions of Fission Fragments in 13-MeV Proton-Induced Fission of ^{232}Th

T. Ohtsuki,[1] Y. Nagame,[2] H. Ikezoe,[2] K. Tsukada,[1] K. Sueki,[1] and H. Nakahara[1]

[1]Department of Chemistry, Faculty of Science, Tokyo Metropolitan University, Fukasawa, Setagaya, Tokyo 158, Japan

[2]Japan Atomic Energy Research Institute (JAERI), Tokai, Ibaraki 319-11, Japan

(Received 21 August 1990)

In the proton-induced fission of ^{232}Th, a binary structure was observed in the velocity and the total-kinetic-energy distributions of fission fragments with $A = 128$-131. From the present results, it is concluded that there are at least two kinds of scission configurations: elongated shapes probably associated with the symmetric liquid-drop path, and more compact shapes associated with the asymmetric shell-influenced path.

Recent data for the total-kinetic-energy distributions in the low-energy fission of the heavy nuclides such as ^{258}Fm, ^{258}No, ^{259}Md, ^{260}Md, and ^{262}No reveal the existence of two types of scission configurations for the same symmetric mass division:[1,2] a compact shape corresponding to the observed high total kinetic energy of about 235 MeV and an elongated shape to that of about 200 MeV. Hulet et al.[1] have called such phenomena "bimodal" fission. A similar report on the existence of multicomponents in the total-kinetic-energy distribution of fragments with $A = 132$-137 has been published by Soviet workers[3] for the fission of preactinides, although their data suffer from poor statistics and need further confirmation. Understanding of the phenomena has been attempted by theoretical calculations of the potential-energy surface of extremely deformed nuclei which show two paths leading to scission[4,5] in the fission of those heavy nuclides. The existence of two fission valleys in the potential-energy surface has also been predicted even for lighter actinide nuclei and for preactinides by some theorists,[6-8] although proper dynamical consideration still remains to be given. "Two modes" of fission was first suggested by Turkevich and Niday[9] to explain the marked decrease of the peak-to-valley ratios of the mass distributions with increasing excitation energy. Such a two-modes hypothesis has been supported by the observation of various different behaviors of symmetrically and asymmetrically divided products of fission, such as incident-energy dependence of mass yields,[10,11] fragment angular distributions,[12] and fragment kinetic energies.[13] The aim of the present work is to measure, by the double time-of-flight method, velocities and kinetic energies of fragments produced in the proton-induced fission of ^{232}Th, and to investigate if there are two components in the time and kinetic-energy distributions of fragments with the mass in the region of $A = 126$-132 where both symmetric and asymmetric modes are expected.

The target of ^{232}Th was evaporated on a 10-μg/cm^2 carbon foil and the thickness was estimated to be 45 μg/cm^2. A beam of 13-MeV protons from the JAERI tandem accelerator was used for the bombardment. At this energy, the reaction is expected to be sub-Coulomb and the fission cross section was shown to be 200 mb by Kudo et al.[11] The beam current was about 500 nA. The measurement of velocities of fission fragments was made by two time-of-flight (TOF) telescopes placed at 45° and $-133.5°$ with respect to the beam direction in order to take into consideration the kinematical deviation. A microchannel plate (MCP) equipped with a carbon foil (30 μm) gave start signals and a parallel-plate avalanche counter (PPAC) gave stop signals. The flight paths were 82.0 and 60.7 cm with the detection solid angles of 0.1 and 2 msr, respectively. The flight times of each of the pair fragments in coincidence was accumulated event by event with an 8192-channel analog-to-digital converter and recorded in a host computer. Altogether 1.5×10^5 fission coincidence events were accumulated in one run. The coincidence rate for a pair of fission fragments was over 80% of the total single events detected by the counter of the smaller geometry. The velocity calibration was performed with a time calibrator and a ^{252}Cf source whose average velocities of the light and heavy fragments have been accurately measured by many groups.[14,15] The primary mass (before neutron emission) of a fission fragment was obtained from the ratio of the two velocities of the pair fragments with assumptions that no neutron was emitted from the compound nucleus prior to fission [at $E_p = 13$ MeV, (p,f) and (p,nf) are energetically allowed and it is likely that (p,f) is the predominant channel according to the previous analysis of the excitation function of fission[11]] and that the neutrons from the primary fragment were isotropically emitted and did not alter the initial fragment velocity on the average:

$$m_1 = M(1 + v_1/v_2)^{-1}, \qquad (1)$$

where M denotes the mass of the fissioning nuclide and v_1 and v_2 are velocities of the pair in the center-of-mass system. The kinetic energies of fission fragments were
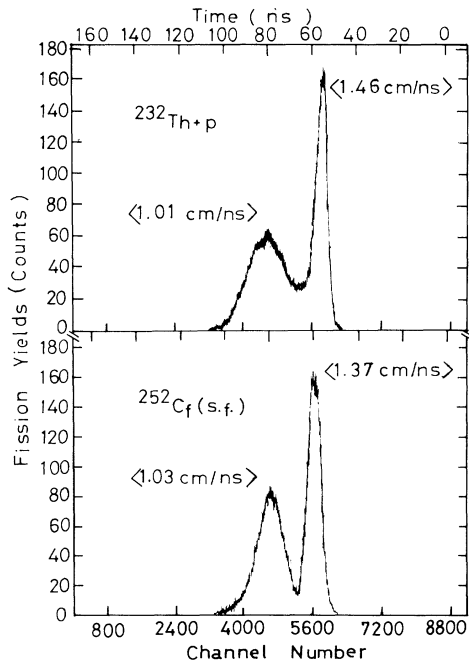
FIG. 1. Fission-fragment time distribution of ^{232}Th$+p$ as a function of channel number and the time scale for the 82.0-cm flight path, and that of ^{252}Cf spontaneous fission.

easily calculated from the mass and velocity as

$$E_{KEi} = \tfrac{1}{2} m_i v_i^2, \quad i = 1, 2. \tag{2}$$

Before carrying out the above analysis, the TOF data were corrected for the velocity loss caused by the target material, the carbon foil of the MCP, and the window of the PPAC by use of the energy-loss relationship.[16] The resulting fragment-mass resolution was estimated to be $\sigma(m) \sim 1.5$ u, mainly based on the resolution of the time measurement and the difference in the flight path depending on the emission angle.

The coincidence TOF spectra of the ^{232}Th$+p$ fission are shown in Fig. 1 together with those of ^{252}Cf spontaneous fission for comparison. The average velocities of the light and the heavy fragments of the ^{232}Th$+p$ fission were 1.46×10^9 and 1.01×10^9 cm/s, respectively. The primary mass-yield distribution for the ^{232}Th$+p$ fission is shown in Fig. 2 whose shape is typically asymmetric, and has a broad symmetric region as expected. The average total kinetic energy $\langle$TKE$\rangle$ and the variance σ_{TKE} for each mass split are shown in Figs. 3(a) and 3(b) as a function of the heavier fragment mass. The peak of $\langle$TKE$\rangle$ falls at around mass 131-132, and that of σ_{TKE} shift toward the lighter-mass side, namely, at 127-128. The average total kinetic energy (TKE) was 168.2 MeV which was in agreement with the Viola's systematics.[17] In Fig. 3(c), the skewness of the total-kinetic-energy distribution defined as

$$\sum_i (TKE_i - \langle TKE \rangle)^3 \Big/ \sigma_{TKE}^3 \tag{3}$$

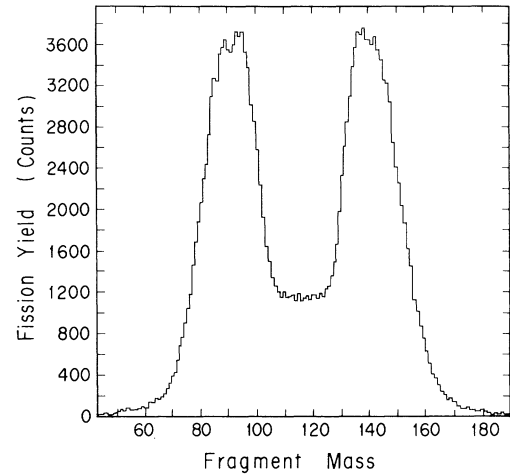for each mass split is shown as a function of the heavy fragment mass. It is found that the value takes a large negative value between the fragment mass 136 and 139. It is interesting to note that the skewness remains constant in the mass region 142-146 and approaches zero as the fragment mass is further increased.

The time distribution (left-hand side) for the 82.0-cm flight path and the corresponding total-kinetic-energy distribution (right-hand side) of each fragment mass are shown in Fig. 4 for the region $A = 126$-132. The shapes
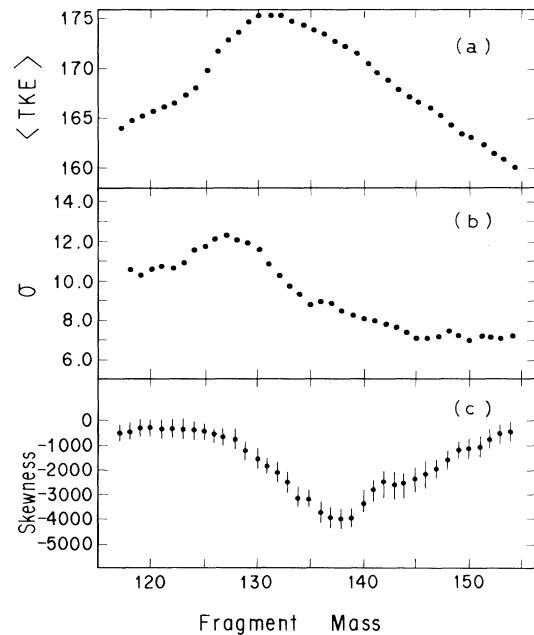

FIG. 2. Fission-fragment mass distribution of ^{232}Th$+p$ for 13.0-MeV protons.

FIG. 3. (a) Observed average-kinetic-energy distribution ($\langle$TKE$\rangle$), (b) the variance (σ), and (c) the skewness for each fragment mass.
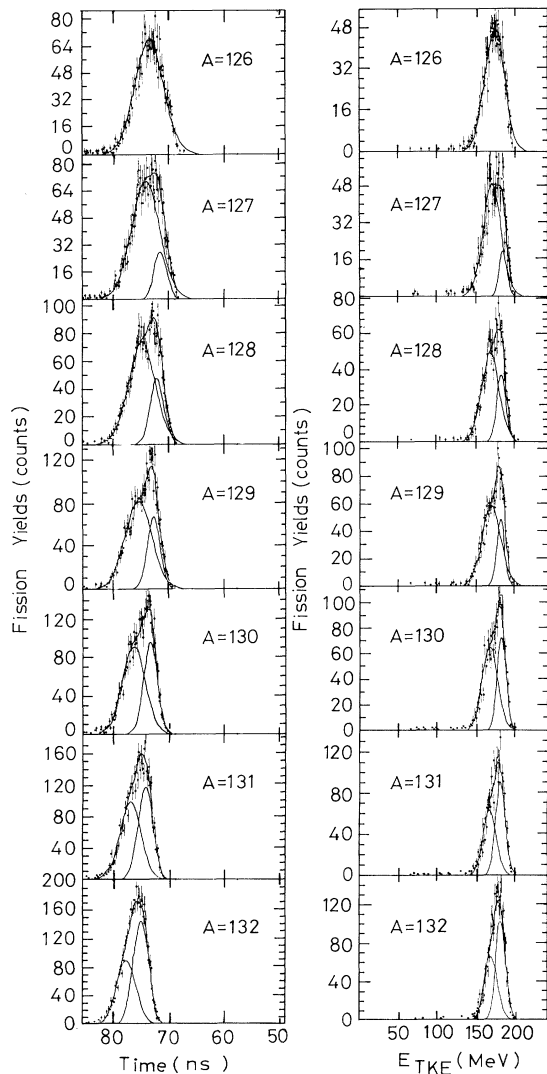
FIG. 4. Time distributions for the 82.0-cm flight path and the total-kinetic-energy distributions in the fragment-mass region $A = 126$–132. Solid curves indicate the result of a Gaussian fit to the time and energy distributions.
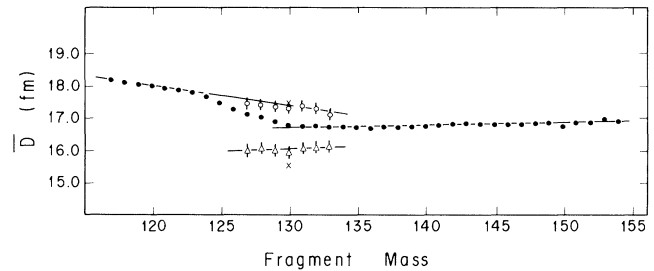

FIG. 5. Distance of the two charge centers at scission configuration evaluated from the total kinetic energy of each fragment mass. The solid circles show the distances calculated from the mean-total-kinetic-energy distribution, open circles and open triangles indicate the distances corresponding to the two types of kinetic-energy distributions (the error bars were estimated from the time resolution and the Gaussian fitting errors), and crosses for the distances of the low and high kinetic-energy components evaluated from the report on ^{258}Fm spontaneous fission [presented by Hulet and co-workers (Refs. 1 and 2)].

of the distributions change systematically, namely, the distribution is nearly symmetric for $A = 126$, clearly double peaked for $A = 128$ and with a shoulder at the left side of the time distribution (lower side of the energy distribution) for the larger fragment mass of $A = 129$–131. A similar systematic change of the shape of the time and energy distributions with the binary structure was observed for the complementary light-mass fragments. The same trend could be observed even when they were plotted as a function of the sum of two neighboring fragment masses. In other mass regions, no clear binary structure was observed in the time distribution. These observations are certainly unaffected by the ambiguity of the mass of the fissioning nuclide by one unit,

namely, ^{233}Pa or ^{232}Pa. Three runs were repeated to confirm the result and the presence of the binary structure in the time distribution was observed in every run; but a broad single peak was observed when thick targets (more than 100 μg/cm^2) with a larger detection geometry were used. This new finding indicates that there exist two kinds of the time and energy distributions for the same mass split at least in the region $A = 128$–131 where the dispersion of the total-kinetic-energy distribution is the largest. Although the time and energy distributions for each fragment mass may not necessarily be of Gaussian shape, the observed distributions were analyzed, as a first approximation, by two Gaussians for the fragment mass $A = 127$–133, and the peak position and the area of each Gaussian were estimated. In terms of the total kinetic energy, the peak positions of the two Gaussians were about 169 and 185 MeV for $A = 128$. The average difference of the two peaks was almost 16 MeV over the region $A = 127$–133. With an assumption of the total kinetic energy originating purely from the Coulombic repulsion between the two fragments at the scission point, the distance (D) between the two charge centers of the complementary fragments was evaluated for the peak energy of each Gaussian distribution, and plotted in Fig. 5 by open symbols: circles for the lower energy and triangles for the higher energy in the mass region $A = 127$–133. The solid circles in the figure show the distance calculated for the mean total fragment kinetic energy. The distance for the high-energy component (open triangles) gradually increases with the increase of the fragment mass while that for the low-energy component (open circles) decreases. It is also to be noted that the open circles lie on the straight line drawn through the solid circles for the more symmetrically divided products while the line drawn through the open triangles stays rather parallel to the line drawn

19

through solid circles for more asymmetrically divided products. These trends of the distance between the two charge centers suggest the presence of at least two distinctively different scission configurations; elongated shapes probably associated with more symmetric mass division and compact shapes associated with asymmetric mass division. The compact shapes found in the mass region $A = 127-133$ can be different from those expected from an extrapolation of more asymmetrically divided products, and they may correspond to what Brosa calls "standard I."[8] But as a Gaussian shape has been assumed in the present analysis, any conclusive statement will not be made at the present stage.

Finally, the distances between the two charge centers corresponding to the "bimodal fission" reported for the spontaneous fission of ^{258}Fm are plotted by crosses in Fig. 5. Surprisingly, they lie close to the open symbols of the present result, although the distance for a compact shape is smaller for the former, possibly due to the $N = 82$, $Z = 50$ shell effect on both of the complementary fragments of ^{258}Fm. This similarity points out that the bimodal fission is not a phenomena peculiar to very heavy nuclides such as ^{258}Fm and ^{260}Md, but that it is also observed in the low-energy proton-induced fission of ^{232}Th; namely, there are essentially at least two different deformation paths in fission, the liquid-drop path which ends up with an elongated scission configuration and favors symmetric mass division, and the shell-influenced path throughout the fission process which causes a compact scission and favors the production of fragments with $A = 130-140$ (at higher excitation energy of 50–70 MeV, washing out or diminishing of the shell effects is predicted,[18] but at the excitation energy of about 20 MeV, as in the case of the 13-MeV proton-induced fission of the present work, the shell effects may not differ much from those on the spontaneous-fission process).

[1]E. K. Hulet, J. F. Wild, R. J. Dougan, R. W. Lougheed, J. H. Landrum, A. D. Dougan, M. Schädel, R. L. Hahn, P. A. Baisden, C. M. Henderson, R. J. Dupzyk, K. Sümmerer, and G. R. Bethune, Phys. Rev. Lett. **56**, 313 (1986).

[2]E. K. Hulet, in *Proceedings of the Fifty Years with Nuclear Fission, Washington, D.C. and Gaithersburg, Maryland, 1989*, edited by J. W. Behrens and A. D. Carlson (American Nuclear Society, Inc., La Grande Park, IL, 1989), Vol. 2, p. 533.

[3]M. G. Itkis, V. N. Okolovich, A. Ya. Rusanov, and G. N. Smirenkin, Z. Phys. A **320**, 433 (1985).

[4]P. Möller, J. R. Nix, and W. J. Swiatecki, Nucl. Phys. **A469**, 1 (1987).

[5]S. Ćwiok, P. Rozmej, A. Sobiczewski, and Z. Patyk, Nucl. Phys. **A491**, 281 (1989).

[6]V. V. Pashkevich, Nucl. Phys. **A169**, 275 (1971).

[7]J. F. Berger, M. Girod, and D. Gogny, Nucl. Phys. **A428**, 23c (1984).

[8]U. Brosa, S. Grossmann, and A. Müller, Z. Phys. A **325**, 241 (1986).

[9]A. Turkevich and J. B. Niday, Phys. Rev. **84**, 52 (1951).

[10]T. Ohtsuki, Y. Hamajima, K. Sueki, H. Nakahara, Y. Nagame, N. Shinohara, and H. Ikezoe, Phys. Rev. C **40**, 2144 (1989).

[11]H. Kudo, H. Muramatsu, H. Nakahara, K. Miyano, and I. Kohno, Phys. Rev. C **25**, 3011 (1982).

[12]H. Kudo, Y. Nagame, H. Nakahara, K. Miyano, and I. Kohno, Phys. Rev. C **25**, 909 (1982).

[13]H. C. Britt, H. E. Wegner, and J. C. Gursky, Phys. Rev. **129**, 2239 (1963).

[14]H. Henschel, A. Kohnel, H. Hipp, and G. Gönnenwein, Nucl. Instrum. Methods Phys. Res. **190**, 125 (1981).

[15]H. W. Schmitt, W. E. Kiker, and C. W. Williams, Phys. Rev. **137**, B837 (1965).

[16]J. F. Ziegler, J. P. Biersack, and U. Littmark, in *Stopping and Range of Ions in Solids*, edited by J. F. Ziegler *et al.*, Stopping and Ranges of Ions in Matter Series Vol. 1 (Pergamon, New York, 1985).

[17]V. E. Viola, K. Kwiatkowski, and M. Walker, Phys. Rev. C **31**, 1550 (1985).

[18]V. Strutinsky, Nucl. Phys. **A502**, 67c (1989).